JOURNAL OF Materials CHEMISTRY

Transformation of porous doped silica xerogels into multicomponent bulk amorphous monoliths with interesting optical properties†

Valerij S. Gurin,*[a] Vitali B. Prokopenko,[b] Alexander A. Alexeenko[c] and Anatoly V. Frantskevich[d]

[a]*Physico-Chemical Research Institute, Belarusian State University, Minsk 220080, Belarus. E-mail: gvs@fhp.bsu.unibel.by; gurinvs@usa.net*
[b]*Gomel State University, Gomel 246699, Belarus*
[c]*Gomel State Technical University, Gomel 246746, Belarus*
[d]*Belarusian State University, Minsk, Belarus*

Received 19th May 2000, Accepted 18th July 2000
First published as an Advance Article on the web 19th October 2000

We have developed a technique for the fabrication of glassy silica materials with ultrafine metal and semiconductor particles. The porosity of xerogels produced under incomplete polycondensation strongly influences the chemical state of the final products, which are formed by reactions of xerogel-dopants in different atmospheres. We have studied, in particular, the process leading to copper sulfide and copper selenide nanoparticles which are promising for non-linear optical applications due to the appearance of a new absorption band in the near IR.

1.0 Introduction

Porous solids have a number of unique properties due to their large active interface with the atmosphere and the peculiar structure of pores usually formed spontaneously[1,2] or by means of some lithographic method.[3] They can be both inert supports (*e.g.*, containing a catalyst for reactions with gaseous or liquid components) and play an active role, providing chemical processes with participation of species bound to the material (*e.g.*, ion-exchange in zeolites). Silica is one of a number of porous solids and has been extensively studied for different purposes, however, there are still unresolved questions even in this quasi-monocomponent material. An ideal chemical structure with tetrahedral SiO_4 groups is not an adequate representation of any porous silica because of its amorphous character and numerous surface hydroxyl groups arising either from synthesis or chemisorbed from the atmosphere. Meanwhile, the porosity allows the combination of silica with a wide variety of other components which may be introduced into the pores with further conversion into a desired dense state. One such procedure which combines porous silica and transition metal ions was designed by us for the fabrication of optical materials with unique optical properties. Fortunately, silica is very suitable for applications in optics due to its good transparency through the UV/Vis/near IR range, and its chemical reactivity is low enough to avoid any chemical interaction of the matrix with dopants. The familiar sol–gel process[4–6] includes a porous silica xerogel step which provides a useful method for silica doping and modification. Conditions of further transformations allow control of the chemical state of such an X-SiO_2 material. As X in this paper we considered copper, copper oxides and chalcogenides; however, many other elements and compounds (each requiring suitable conditions) could be analogously introduced into the porous silica xerogel. One other exciting feature of this process is the production of dopants in the form of small particles dispersed within the silica matrix: the particles can be metallic or semiconducting comprising "nanoparticles-in-dielectrics" materials with quantum confinement effects in the nanoparticle properties and particle–particle interactions.[7–9]

The purpose of the present work was the fabrication of multicomponent silica-based solid materials through porous xerogels with ultrafine copper compounds, and study of their structural and optical properties. The materials fabricated are of interest, in particular, for optical element applications, and the method presented allows variation of their characteristic features for the construction of filters, non-linear switches, and optical limiters. Fabrication routes and some physical properties of sol–gel derived silica materials with copper and copper oxides were reported previously for monolithic compositions[10–13] and films;[14,15] however, our research was aimed at materials with semiconductor copper chalcogenide particles produced in a glassy optically transparent silica matrix rather than every CuX–SiO_2 nanocomposite.

2.0 Preparation and further processing

The complete cycle of the sol–gel procedure of multicomponent matrix formation (from liquid sol to stiff transparent glass) partially repeats the familiar routes[16–21] which were suggested for optical materials doped with small semiconductor particles; however, fabrication of the sol–gel glasses with copper chalcogenides was performed by us for the first time and published in ref. 22. The preparation route includes the following sequence of steps. The precursor solution was prepared by mixing of tetraethoxysilane (TEOS), water, and HCl (mole ratio 1 : 25 : 0.05, respectively). In order to overcome a strong volume contraction during gel drying, aerosil with a particle size of 15–20 nm was added to the sols. It should be noted that approx. 50% contraction remained with the aerosil present, but in its absence no stiff and crack-free xerogels could be obtained with the given procedure. After mixing and stirring for 1 h, ultrasonic activation and removal of agglomerates from the sol by centrifugation, aqueous ammonia was added to increase the pH of the sol to 7–8. Then this sol was poured into closed polystyrene containers and left for a day for gelation. Gels were heated at 800 °C for 1 h and uniform porous samples in the form of disks were produced. These xerogels were used as initial starting materials for the preparation of samples doped with different copper compounds. Copper was introduced into the xerogels by impregnation in alcoholic solutions of $Cu(NO_3)_2$ for 8 h. Impregnated doped xerogels were dried in air and heated at 600 °C for 1 h. The next operations with the

†Basis of a presentation given at Materials Discussion No. 3, 26–29 September, 2000, University of Cambridge, UK.

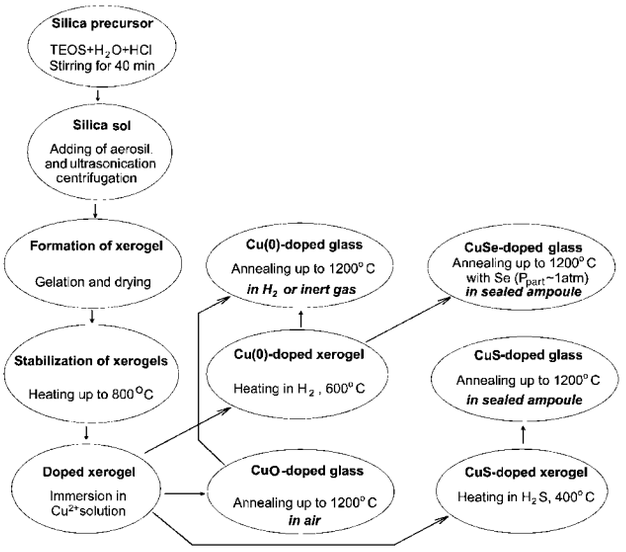

Fig. 1 The preparation sequence of silica monoliths doped with metallic copper, copper sulfide, copper oxide and copper selenide. A detailed description of each step is given in the text.

copper-doped xerogels included one of the routes described below, and shown schematically in Fig. 1.

(i) Annealing in air at a maximum temperature of 1200 °C (for 10 min) led to the formation of a transparent light-brown glass. The subsequent heating of the sol–gel glass was carried out in flowing hydrogen at 600 °C for 1 h. As a result of such treatment the light-brown glasses were transformed into red transparent glasses. Analogous materials were obtained in one step after the high-temperature annealing of the copper-doped xerogels in flowing hydrogen (Fig. 1).

(ii) Heating in flowing hydrogen (600 °C for 1 h) followed by annealing in closed quartz ampoules (ampoule volume 10–20 times greater than sample volume) together with a small amount of elemental selenium. The amount of selenium was calculated to provide a partial pressure of Se vapour of about 1 atm at the maximum temperature of the heat treatment (1200 °C). The ampoules were sealed without any outgassing of air. The xerogels in the closed ampoules were heated to 600 °C, held for 1 h at this temperature and further heated to 1200 °C with a temperature ramp rate of 100 °C h^{-1}, and finally heated at 1200 °C for 10 min. As a result of this sequence the xerogels resulting from treatment (i) were also transformed into transparent dark-green glassy samples.

(iii) Heating in flowing hydrogen sulfide (400 °C for 1 h) followed by annealing in sealed quartz ampoules similarly to treatment (ii), but without selenium. The ampoules were also sealed without any outgassing and heated by the same temperature regime to 1200 °C. This route resulted in transparent dark-brown glassy samples. All glasses fabricated were polished to an appropriate thickness for optical measurements. Thus, we studied four types of glassy samples (monoliths) transformed from Cu-doped xerogels: oxidized, hydrogen reduced, selenized and sulfidized. We expected the appearance of copper oxide, metallic copper, copper selenide and copper sulfide, respectively, within these materials after the above described procedures.

3.0 Results and discussion

3.1. X-Ray diffraction

The glassy materials under study were produced *via* the transformation of a porous xerogel into a transparent glassy monolith. This transformation is inherent to the pure xerogels which were not doped with copper or with any other component. A dopant is required to be inert at the loading used (the admissible maximum amount has been established experimentally and in the typical samples presented was 0.5–1 at.%). Note that the annealing process can be changed completely when higher amounts of dopant are used. We kept a low dopant amount, and the heating and annealing regimes were same for the doped and pure xerogels. These regimes resulted in the formation of high optical quality, transparent samples in the final steps. This allowed us to study the annealing process with pure xerogels. In other words, it was assumed that the behaviour of the silica matrix of the pure xerogels is same as in the doped ones. X-Ray diffraction (XRD) analysis was carried out for a series of xerogels heated under different temperatures (600–1250 °C) (Fig. 2). The first set of XRD data (Fig. 2a) characterizes xerogels during the pre-annealing steps: they remain very porous and no volume contraction occurred. The second set (Fig. 2b) corresponds to the annealing observable by the naked eye: a volume contraction (up to 50%) with conservation of the initial shape (*i.e.* the samples were not melted) and the appearance of transparency, with an optical spectrum similar to fused silica glass formed by traditional methods. These diffractograms exhibit the well-known broad peak of amorphous silica, the position of which is practically identical for both sets of xerogels (*i.e.* those heated to 600–1000 °C and 1100–1250 °C). The maximum of this peak appears at $2\theta = 23°$ with a peak width from 15 through 30°; it originates from the disordered –O–Si–O– network of the amorphous material and may be related to the contribution from the first and second neighbouring Si atoms. The degree of this disorder is slightly increased in the xerogels from 600 to 1000 °C, and it is retained under the different steps of annealing. No traces of crystallization were observed at this temperature. The cristobalite phase of SiO_2 was formed only after heat treatment at 1500 °C (not shown in Fig. 2). It should be kept in mind that the radial distribution function of atoms may not be evaluated from wide-range XRD, however, the data suggest that the local structure of silica does not change significantly. The annealed xerogels are the same amorphous material as the porous one. The annealing process only results in a decrease in the pore volume (until the disappearance of the pores).

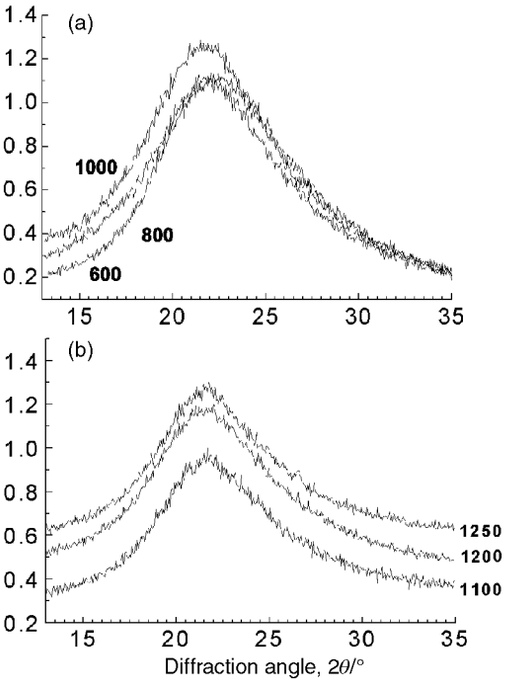

Fig. 2 A series of X-ray diffraction data in the range of $2\theta = 15–35°$ for the pure silica xerogels and monoliths (*i.e.* annealed xerogels) without any doping after heating at different temperatures (specified on the curves) for 1 h. The ordinate is given in arbitrary units.

Note that the Cu-doped annealed xerogels have similar diffractograms: the amount of copper atoms in silica glass is probably too small to be detectable with XRD, but the local silica structure has not been appreciably changed by the presence of copper.

3.2. Optical spectroscopy

As the result of the xerogel-to-glass transformation according to route (iii), coloured glassy samples were obtained which were studied with optical absorption spectroscopy. Fig. 3 displays typical spectra for the four kinds of materials synthesised. The almost structureless curve (1) corresponds to the copper oxide step. It is similar to the spectra of this compound dispersed in films and glasses[23,24] and compatible with the indirect band-gap character of this semiconductor; E_g is estimated to be 1.4–1.5 eV.[25,26] A rather pronounced feature is observed for the hydrogen-reduced monoliths (curve 2, Fig. 3). A peak at 2.1 eV with a shoulder in the range of 1.7–1.8 eV is typical for ultrafine copper particles exhibiting a plasmon resonance[27] just in this region. Copper particles with a well-expressed plasmon resonance have been produced within oxide matrices.[11,28–30] The exact shape of the resonance depends on the size and sphericity of the particles and their interactions with the matrix and environment. The latter may be responsible for the low-energy part of this feature. As a result of sulfidization and selenization of copper oxide and copper, respectively, with subsequent annealing, we obtained absorption spectra comprising two parts: a monotonous absorption rise in the high-energy part with the appearance of the broad band for selenide samples, and a broad maximum in the low energy part (curves 3 and 4 in Fig. 3). The maximum corresponding to sulfide was located at about 1.9 eV, and in the case of selenide it is shifted to the near-IR region, 1.1 eV. This rather different position of the maximum could not be associated with formation of copper ions in the glasses under annealing, absorption of these covers the range 1.5–2.0 eV,[11,31,32] since we observe the explicit effect of chalcogen type species. The interpretation of this effect as arising from the absorption of ultrafine copper selenide and sulfide particles is more likely. The fundamental absorption edges of sulfides with different stoichiometries were determined to be from 1.2 eV for Cu_2S[33,34] to 2 eV for CuS.[35,36] For copper selenides the data on E_g vary from 1.4 to 2.2 eV, depending on the preparation details and the stoichiometry.[37,38] For copper sulfides the properties of quantum-size particles with a similar maximum were reported in refs. 39–41. These data support the conclusion drawn on the appearance of copper sulfide particles in our case. The near-IR absorption for selenide cannot be treated as a quantum-size effect, which would result in a blue-shift rather than the red-shift observed here. A contribution from quantum-sized selenide particles can be considered to explain the band between 2.0 and 2.5 eV, but the near-IR maximum has, perhaps, another origin. Analogously with the properties of the sol–gel silica films containing copper selenide (for different stoichiometry, Cu_xSe, $1 \leqslant x \leqslant 2$) we propose a partial oxidation of the particles with the formation of interband levels responsible for transitions with an energy of about 1.1 eV. A large surface/volume ratio in the case of ultrafine particles provides the considerably high intensity of this maximum.

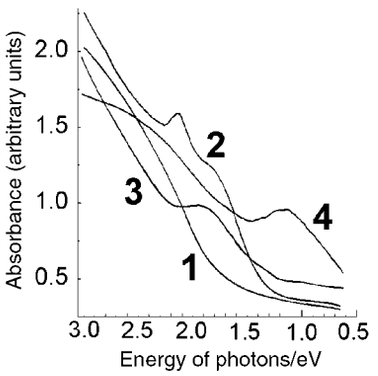

Fig. 3 Absorption spectra of the four types of Cu-doped silica monoliths obtained at the steps of formation of metallic copper (2), and copper compounds: CuO (1), Cu_xS (3), and Cu_xSe (4).

3.3. Transmission electron microscopy

From the optical data we can conclude that the different chemical compositions of the glasses produced by means of chemical transformations of a series of copper compounds reveal very distinct optical absorption properties. The interpretation of this fact given above as arising from the occurrence of nanoparticles was confirmed directly with transmission electron microscopy (TEM). The micrographs were obtained by means of the 'replica with extraction' method (a carbon film of 10 nm thickness was evaporated onto slightly etched samples and was separated at the water–air interface by careful immersion into water and transferred onto standard TEM copper meshs). They indicate unambiguously that the colour of the glasses is controlled by particles which are present in rather low concentrations, 10^{13}–10^{14} cm^{-3} (the amount of matter is in agreement with the optical absorption intensity). The particles are near-spherical and their average sizes are collected in Table 1. These data indicate that the range of particle sizes is similar in glasses of different compositions, apart from CuO/SiO_2 for which the presence of some amorphous phase cannot be excluded. Optical spectra for this glass did not reveal any pronounced features. In the semiconductor-doped, Cu_xS/SiO_2 and Cu_xSe/SiO_2 materials the size of the particles could contribute only as a weak quantum confinement effect (since typical values of the Bohr radius of similar medium-band chalcogenide semiconductors are less than 10 nm[42,43]). Thus, the multicomponent materials fabricated can be related to the particles-in-dielectric matrix systems with explicit separation of the component features.

3.4. Rutherford backscattering spectroscopy

It should be noted that full analysis of the chemical compositions of similar composites is very complicated: any destructive methods result in strong distortion of data since the nanoparticles are not stable in the absence of a glass matrix or some other protective shell. Our preliminary conclusions on the composition issue, first of all, from the analogous data on the Cu_xS– and Cu_xSe–silica films, were obtained with XRD and X-ray photoelectron spectroscopy (XPS) studies.[44,45] For the latter, Cu_xSe/SiO_2, the optical properties of the films and glasses considered in the present work are similar, and we performed additional compositional studies with Rutherford backscattering spectroscopy (RBS; Table 2).

A typical experimental setup was used: the 1.6 MeV $4He^{2+}$ beam incident normally on the samples was detected at a scattering angle of 160°. The data on the elemental composition

Table 1 Averaged sizes of nanoparticles formed in the monoliths according to TEM data

Type of monolith	Particle size/nm
Cu/SiO_2	20–50
CuO/SiO_2	No particles were observed[a]
Cu_xS/SiO_2	30–100
Cu_xSe/SiO_2	20–80

[a]Under the above TEM observation using the "replica with extraction" method we did not detected with any certainty particles less than 5–10 nm; however, other studies of these samples (kindly performed by Dr. Shixin Wang, Michigan University) with HRTEM have confirmed the absense of explicit crystalline phases in these monoliths.

Table 2 Data of RBS analysis of Cu_xSe-containing silica monoliths within the surface layer of a freshly cleaved sample

Element	Relative amounts (atom%)
O	67.82
Si	32.00
Cu	0.13
Se	0.06

indicate that the stoichiometry of the copper selenide formed was Cu_2Se, whilst a different selenization extent can provide a range of selenides Cu_xSe with controllable x value within the silica films.[46,47] Thus, the analysis performed showed that the properties of these multicomponent semiconductor–glass materials can be controlled both *via* the type of copper compound and the stoichiometry of the chalcogenides. The last circumstance is inherent to transition metal compounds and is unknown for the classical semiconductor-doped glasses with $A^{II}B^{VI}$, $A^{III}B^{V}$, and $A^{IV}B^{VI}$ compounds. The size effect, which is much more usable for control of glass properties,[7,8,43,48] was not investigated by us within the framework of this work, and will be the subject of further studies.

4.0 Conclusions

1. A series of monolithic silica glasses doped with different copper compounds (oxide and chalcogenides) and metallic copper was fabricated with the sequence of steps including the sol–gel process, heating and annealing of porous xerogels in controllable atmosphere for *in situ* chemical transformations.

2. Ultrafine metallic copper, copper sulfide and copper selenide nanoparticles were formed within the silica matrix at the final annealing step, accompanied by the transformation of porous xerogels to glasses. The particles, with sizes in the range of tens of nanometers, which are separately located in the matrix provide unusual optical properties of the materials.

3. The copper selenide doped glasses are of greatest interest for optical applications since they possess an intense near-IR absorption band. Their composition was determined as Cu_2Se/SiO_2; however, control of the size of particles and stoichiometry of Cu_xSe may be feasible in order to tune the unique optical non-linear properties.

Acknowledgements

The authors thank Drs. A. S. Lyakhov and L. S. Ivashkevich for assistance in XRD measurements and Dr. K. V. Yumashev and P. V. Prokoshin for recording of absorption spectra in the near-IR range. This work was supported by the Belarusian Fundamental Foundation and Ministry of Education of Belarus.

References

1 *Access in nanoporous materials*, ed. T. J. Pinnavaia and M. F. Thorpe, Kluwer Acadademic Publishers, Dordrecht, The Netherlands, 1996.
2 C. N. R. Rao, *J. Mater. Chem.*, 1999, **9**, 1.
3 Y. Xia, J. A. Rogers, K. E. Paul and G. M. Whitesides, *Chem. Rev.*, 1999, **99**, 1823.
4 D. R. Ulrich, *J. Non-Cryst. Solids*, 1988, **100**, 174.
5 L. L. Hench and J. K. West, *Chem. Rev.*, 1990, **90**, 33.
6 J.-L. R. Nogues and W. V. Moreshead, *J. Non-Cryst. Solids*, 1990, **121**, 136.
7 F. Henneberger and J. Puls, in *Optics of Semiconductor Nanostructures*, Academie Verlag, Berlin, 1992, p. 497.
8 N. R. Kulish, V. P. Kunets and M. P. Lisitsa, *Opt. Eng.*, 1995, **34**, 1054.
9 L. L. Beecroft and Ch. K. Ober, *Chem. Mater.*, 1997, **9**, 1302.
10 M. G. Ferreira Da Silva and J. M. Fernandez Navarro, *J. Non-Cryst. Solids*, 1988, **100**, 447.
11 J. F. Perez-Robles, F. J. Garcia-Rodriguez, J. M. Yanez-Limon, F. J. Espinoza-Beltran, Y. V. Vorobiev and J. Gonzalez-Hernandez, *J. Phys. Chem. Solids*, 1999, **60**, 1729.
12 A. Mendoza-Galvan, J. F. Perez-Robles, F. J. Espinoza-Beltran, R. Ramirez-Bon, Y. V. Vorobiev and J. Gonzalez-Hernandez, *J. Vac. Sci. Technol. A*, 1999, **17**, 1103.
13 E. M. B. de Sousa, A. O. Porto, P. J. Schilling, M. C. M. Alves and N. D. S. Mohallem, *J. Phys. Chem. Solids*, 2000, **61**, 853.
14 G. De, *J. Sol–Gel Sci. Technol.*, 1998, **11**, 289.
15 G. De, M. Gusso, L. Tapfer, F. Gonella, G. Mattei, P. Mazzoldi and G. Battaglin, *J. Appl. Phys.*, 1996, **80**, 6734.
16 C. J. Brinker and G. W. Scherer, *Sol–gel science: the physics and chemistry of sol–gel processing*, Academic Press, New York, 1990.
17 T. Rajh, M. I. Vucemilovic, N. M. Dimitrijevic, O. I. Micic and A. J. Nozik, *Chem. Phys. Lett.*, 1988, **143**, 305.
18 M. Nogami, S. Suzuki and K. Nagasaka, *J. Non-Cryst. Solids*, 1991, **135**, 182.
19 L. Spanhel, E. Arpac and H. Schmidt, *J. Non-Cryst. Solids*, 1992, **147**(148), 657.
20 P. Lefebvre, T. Richard, J. Allegre, H. Mathieu, A. Pradel, J. L. Marc, L. Boudes, W. Granier and M. Ribes, *Superlattices Microstruct.*, 1994, **15**, 447.
21 O. Levy and L. Esquivias, *Adv. Mater.*, 1995, **7**, 120.
22 V. S. Gurin, V. B. Prokopenko, I. M. Melnichenko, E. N. Poddenezhny, A. A. Alexeenko and K. V. Yumashev, *J. Non-Cryst. Solids*, 1998, **232–234**, 162.
23 M. Ristov, G. Sinadinovski and I. Grozdanov, *Thin Solid Films*, 1985, **123**, 63.
24 R. J. Araujo, J. Butty and N. Peyghambarian, *Appl. Phys. Lett.*, 1996, **68**, 584.
25 J. Ghijsen, L. H. Tjeng, J. van Elp, H. Eskes and M. T. Czyzyk, *Phys. Rev. B*, 1988, **38**, 11322.
26 F. Marabelli, G. B. Parravicini and F. Salghetti-Drioli, *Phys. Rev. B*, 1995, **52**, 1433.
27 U. Kreibig and M. Vollmer, *Optical Properties of Metal Clusters*, Springer, Berlin, 1995.
28 R. H. Magruder III, R. F. Haglund Jr., L. Yang, J. E. Wittig and R. A. Zuhr, *J. Appl. Phys.*, 1994, **76**, 708.
29 P. Mulvaney, *Langmuir*, 1996, **12**, 788.
30 K. Fukumi, A. Chayahara, K. Kadono, H. Kageyama, N. Kitamura, H. Mizoguchi, Y. Horino and M. Makihara, *J. Surf. Anal.*, 1998, **4**, 214.
31 N. I. Vlasova, L. I. Demkina and V. I. Karaseva, *Fiz. Khim. Stekla (St. Petersburg)*, 1984, **10**, 345.
32 C. L. Ballhausen, *Introduction to ligand field theory*, McGraw-Hill Book Company, Inc., New York, 1964.
33 M. J. Mulder, *Phys. Status Solidi (A)*, 1973, **15**, 409.
34 R. Marshall and S. S. Mitra, *J. Appl. Phys.*, 1965, **36**, 3882.
35 P. S. McLeod, L. D. Patrain, D. E. Sawyer and T. M. Peterson, *Appl. Phys. Lett.*, 1984, **45**, 472.
36 N. A. Vlasenko and Ya.F. Kononets, *Ukr. Fiz. Zh.*, 1971, **16**, 237.
37 K. L. Chopra and S. R. Das, *Thin Film Solar Cells*, Plenum Press, New York, 1983.
38 G. P. Sorokin, Yu. M. Papshev and P. T. Oush, *Fiz. Tverd. Tela (St. Petersburg)*, 1965, **7**, 2245.
39 V. I. Klimov, P. H. Bolivar, H. Kurz, V. Karavanskii, V. Krasovskii and Yu. Korkishko, *Appl. Phys. Lett.*, 1995, **67**, 653.
40 V. I. Klimov, P. H. Bolivar, H. Kurz and V. Karavanskii, *Superlattices Microstruct.*, 1996, **20**, 399.
41 V. I. Klimov and V. A. Karavanskii, *Phys. Rev. B*, 1996, **54**, 8087.
42 A. D. Yoffe, *Adv. Phys.*, 1993, **42**, 173.
43 S. V. Gaponenko, *Optical properties of semiconductor nanocrystals*, Cambridge University Press, Cambridge, 1998.
44 V. S. Gurin, V. B. Prokopenko, A. A. Alexeenko, D. L. Kovalenko and I. M. Melnichenko, *J. Inclus. Phenom. Macrocycl. Chem.*, 1999, **35**, 291.
45 V. S. Gurin, V. B. Prokopenko, A. A. Alexeenko, I. M. Melnichenko, V. P. Mikhaolov, K. V. Yumashev and A. M. Malyarevich, *Funct. Mater. (Kharkov)*, 1999, **6**, 464.
46 Z. Vucic, O. Milat, V. Horvatic and Z. Ogorelec, *Phys. Rev. B*, 1981, **24**, 5398.
47 R. M. Murray and R. D. Heyding, *Can. J. Chem.*, 1975, **53**, 878; R. M. Murray and R. D. Heyding, *Can. J. Chem.*, 1976, **54**, 841.
48 U. Woggon, *Optical Properties of Semiconductor Quantum Dots*, Springer-Verlag, Berlin, Heidelberg, New York, 1997.